

Ab initio computation of the energies of circular quantum dotsM. Pedersen Lohne,¹ G. Hagen,^{2,3} M. Hjorth-Jensen,⁴ S. Kvaal,⁵ and F. Pederiva⁶¹*Department of Physics, University of Oslo, N-0316 Oslo, Norway*²*Physics Division, Oak Ridge National Laboratory, Oak Ridge, Tennessee 37831, USA*³*Department of Physics and Astronomy, University of Tennessee, Knoxville, Tennessee 37831, USA*⁴*Department of Physics and Center of Mathematics for Applications, University of Oslo, N-0316 Oslo, Norway*⁵*Center of Mathematics for Applications, University of Oslo, N-0316 Oslo, Norway*⁶*Dipartimento di Fisica, Università di Trento, and I.N.F.N., Gruppo Collegato di Trento, I-38123 Povo, Trento, Italy*

(Received 26 September 2010; revised manuscript received 21 December 2010; published 8 September 2011)

We perform coupled-cluster and diffusion Monte Carlo calculations of the energies of circular quantum dots up to 20 electrons. The coupled-cluster calculations include triples corrections and a renormalized Coulomb interaction defined for a given number of low-lying oscillator shells. Using such a renormalized Coulomb interaction brings the coupled-cluster calculations with triples correlations in excellent agreement with the diffusion Monte Carlo calculations. This opens up perspectives for doing *ab initio* calculations for much larger systems of electrons.

DOI: [10.1103/PhysRevB.84.115302](https://doi.org/10.1103/PhysRevB.84.115302)

PACS number(s): 73.21.La, 71.15.-m, 31.15.bw, 02.70.Ss

I. INTRODUCTION

Strongly confined electrons offer a wide variety of complex and subtle phenomena, which pose severe challenges to existing many-body methods. Quantum dots, in particular (that is, electrons confined in semiconducting heterostructures), exhibit, due to their small size, discrete quantum levels. The ground states of, for example, circular dots show similar shell structures and magic numbers as seen for atoms and nuclei. These structures are particularly evident in measurements of the change in electrochemical potential due to the addition of one extra electron $\Delta_N = \mu(N+1) - \mu(N)$. Here, N is the number of electrons in the quantum dot, and $\mu(N) = E(N) - E(N-1)$ is the electrochemical potential of the system. Theoretical predictions of Δ_N and the excitation energy spectrum require accurate calculations of ground-state and excited-state energies.

The above-mentioned quantum mechanical levels can, in turn, be tuned by means of, for example, the application of various external fields. The spins of the electrons in quantum dots provide a natural basis for representing so-called qubits.¹ The capability to manipulate and study such states is evidenced by several recent experiments (see, for example, Refs. 2 and 3). Coupled quantum dots are particularly interesting since so-called two-qubit quantum gates can be realized by manipulating the exchange coupling, which originates from the repulsive Coulomb interaction and the underlying Pauli principle. For such states, the exchange coupling splits singlet and triplet states, and depending on the shape of the confining potential and the applied magnetic field, one can allow for electrical or magnetic control of the exchange coupling. In particular, several recent experiments and theoretical investigations have analyzed the role of effective spin-orbit interactions in quantum dots⁴⁻⁷ and their influence on the exchange coupling.

A proper theoretical understanding of the exchange coupling, correlation energies, ground-state energies of quantum dots, the role of spin-orbit interactions, and other properties of quantum dots as well requires the development of

appropriate and reliable theoretical few- and many-body methods. Furthermore, for quantum dots with more than two electrons and/or specific values of the external fields, this implies the development of few- and many-body methods where uncertainty quantifications are provided. For most methods, this means providing an estimate of the error due to the truncation made in the single-particle basis and the truncation made in limiting the number of possible excitations. For systems with more than three or four electrons, *ab initio* methods that have been employed in studies of quantum dots include variational and diffusion Monte Carlo,⁸⁻¹¹ path integral approaches,¹² large-scale diagonalization (full configuration interaction),¹³⁻¹⁶ and to a very limited extent coupled-cluster theory.¹⁷⁻²⁰ Exact diagonalization studies are accurate for a very small number of electrons, but the number of basis functions needed to obtain a given accuracy and the computational cost grow very rapidly with electron number. In practice, they have been used for up to eight electrons,^{13,14,16} but the accuracy is very limited for all except $N \leq 3$ (see, for example, Refs. 15 and 21). Monte Carlo methods have been applied up to $N = 24$ electrons.^{10,11} Diffusion Monte Carlo, with statistical and systematic errors, provides, in principle, exact benchmark solutions to various properties of quantum dots. However, the computations start becoming rather time consuming for larger systems. Hartree,²² restricted Hartree-Fock, spin- and/or space-unrestricted Hartree-Fock²³⁻²⁵ and local spin-density, and current density functional methods²⁶⁻²⁹ give results that are satisfactory for a qualitative understanding of some systematic properties. However, comparisons with exact results show discrepancies in the energies that are substantial on the scale of energy differences.

Another many-body method with the potential of providing reliable error estimates and accurate results is coupled-cluster theory, with its various levels of truncations. Coupled-cluster theory is the method of choice in quantum chemistry, atomic and molecular physics,^{17,18,30} and has recently been applied with great success in nuclear physics as well (see, for example, Refs. 31-34). In nuclear physics, with our spherical basis codes, we expect now to be able to perform

ab initio calculations of nuclei up to ^{132}Sn with more than 20 major oscillator shells. The latter implies dimensionalities of more than 10^{100} basis Slater determinants, well beyond the reach of the full configuration-interaction approach. Coupled-cluster theory offers a many-body formalism that allows for systematic expansions and error estimates in terms of truncations in the basis of single-particle states.³⁵ The cost of the calculations scale gently with the number of particles and single-particle states, and we expect to be able to study quantum dots up to 50 electrons without a spherical symmetry. The main advantage of the coupled-cluster method over, say, full configuration approaches relies on the fact that it offers an attractive truncation scheme at a much lower computational cost. It preserves, at the same time, important features such as size extensivity.

The aim of this work is to apply coupled-cluster theory with the inclusion of triples excitations through the highly accurate and efficient Λ -coupled-cluster singles-doubles (triples) [Λ -CCSD(T)] approach^{36–39} for circular quantum dots up to $N = 20$ electrons, employing different strengths of the applied magnetic field. The results from these calculations are compared in turn with, in principle, exact diffusion Monte Carlo calculations. Moreover, this paper introduces a technique widely applied in the nuclear many-body problem, namely, that of a renormalized two-body Coulomb interaction. Instead of using the free Coulomb interaction in an oscillator basis, we diagonalize the two-electron problem exactly using a tailor-made basis in the center-of-mass frame.¹⁵ The obtained eigenvectors and eigenvalues are used, in turn, to obtain, via a similarity transformation, an effective interaction defined for the lowest 10–20 oscillator shells. These shells define our effective Hilbert space where the coupled-cluster calculations are performed. This technique has been used with great success in the nuclear many-body problem, in particular, since the strong repulsion at short interparticle distances of the nuclear interactions requires a renormalization of the short-range part.^{40,41} With this renormalized Coulomb interaction and coupled-cluster calculations with triples excitations included through the Λ -CCSD(T) approach, we obtain results in close agreement with the diffusion Monte Carlo calculations. This opens up many interesting avenues for *ab initio* studies of quantum dots, in particular, for systems beyond the simple circular quantum dots.

This paper is organized as follows. Section II introduces (i) the Hamiltonian and interaction for circular quantum dots, (ii) the basic ingredients for obtaining an effective interaction using a similarity-transformed Coulomb interaction, then (iii) a brief review of coupled-cluster theory and the Λ -CCSD(T) approach, and finally (iv) the corresponding details behind the diffusion Monte Carlo calculations. In Sec. III, we present our results, whereas Sec. IV is devoted to our conclusions and perspectives for future work.

II. COUPLED-CLUSTER THEORY AND DIFFUSION MONTE CARLO

We present first our Hamiltonian in Sec. II A; thereafter, we discuss how to obtain a renormalized two-body interaction in an effective Hilbert space. In Sec. II C, we present our

coupled-cluster approach, and finally in Sec. II D, we briefly review our diffusion Monte Carlo approach.

A. Physical systems and model Hamiltonian

We will assume that our problem can be described entirely by a nonrelativistic many-electron Hamiltonian \hat{H} , resulting in the Schrödinger equation

$$\hat{H}|\Psi\rangle = E|\Psi\rangle, \quad (1)$$

with $|\Psi\rangle$ being the eigenstate and E the eigenvalue. The many-electron Hamiltonian is normally written in terms of a noninteracting part \hat{H}_0 and an interacting part \hat{V} , namely,

$$\hat{H} = \hat{H}_0 + \hat{V} = \sum_{i=1}^N \hat{h}_i + \sum_{i<j}^N \hat{v}_{ij},$$

where \hat{H}_0 is the (one-body) Hamiltonian of the noninteracting system, and \hat{V} denotes the (two-body) Coulomb interaction. In general, the Schrödinger equation (1) can not be solved exactly.

We define the reference Slater determinant $|\Phi_0\rangle$ as the ground state of the noninteracting system by filling all the lowest-lying single-particle orbits. Since we will limit ourselves to systems with filled shells, this may be a good approximation, in particular, if the single-particle field is the dominating contribution to the total energy. The noninteracting Schrödinger equation reads as

$$\hat{H}_0|\Phi_0\rangle = e_0|\Phi_0\rangle, \quad (2)$$

where

$$\hat{H}_0 = \sum_{i=1}^N \hat{h}_i = \sum_{i=1}^N [\hat{t}_i + \hat{v}_{\text{con}}(\mathbf{r}_i)].$$

The terms \hat{t}_i and $\hat{v}_{\text{con}}(\mathbf{r}_i)$ are the kinetic-energy operator and the confining potential (from an external applied potential field) of electron i , respectively. The vector \mathbf{r}_i represents the position in two dimensions of electron i . Due to the identical and fermionic nature of electrons, the eigenstates of Eq. (2) are Slater determinants, with the general form

$$|\Phi\rangle = |ijk\dots m\rangle = \hat{a}_i^\dagger \hat{a}_j^\dagger \hat{a}_k^\dagger \dots \hat{a}_m^\dagger |0\rangle,$$

with \hat{a}^\dagger being standard fermion creation operators (and \hat{a} being annihilation operators). The single-particle eigenstates $|i\rangle = \hat{a}_i^\dagger |0\rangle$ and eigenenergies ε_i are given by the solutions of the one-particle Schrödinger equation governed by the operator \hat{h}_i . Since the total energy of the noninteracting system is given by the sum of single-particle energies ε_i , we have

$$e_0 = \sum_{i=1}^N \varepsilon_i,$$

the reference determinant $|\Phi_0\rangle$ is obviously the Slater determinant constructed from those orbitals with single-particle energies that yield the lowest total energy. In the particle-hole formalism, orbitals in the occupied space are referred to as hole states, while orbitals in the virtual space are denoted particle states. In principle, any complete and orthogonal single-particle basis can be used. However, since our coupled-cluster approach involves the solution of a set of nonlinear

equations, it is preferable to start from a basis that produces a mean-field solution not too far away from the “exact” and fully correlated many-body solution. Therefore, our main results will be obtained using the Hartree-Fock basis as a starting point for our coupled-cluster calculations. The Hartree-Fock basis is obtained from a linear expansion of harmonic-oscillator basis functions, such that the expectation value of the Hamiltonian is minimized.

For the diffusion Monte Carlo calculations, it is also necessary to start from a model wave function that is used as importance function in the sampling, as we will discuss later. The Slater determinant part, in this case, is built starting from the self-consistent orbitals generated in a local density approximation calculation in order to include as much information as possible about both exchange and correlation effects at the one-body level. Explicit two-body correlations are then included as an elaborate Jastrow factor; see Sec. II D for further details.

Our model Hamiltonian⁴² for a quantum dot consists of a two-dimensional system of N electrons moving in the $z = 0$ plane, confined by a parabolic lateral confining potential $V_{\text{con}}(\mathbf{r})$. The Hamiltonian is

$$\hat{H} = \sum_{i=1}^N \left(-\frac{\hbar^2}{2m_e m^*} \nabla_i^2 + V_{\text{con}}(\mathbf{r}_i) \right) + \frac{e^2}{\epsilon} \sum_{i<j}^N \frac{1}{|\mathbf{r}_i - \mathbf{r}_j|}.$$

In the above equation, m^* is a parameter relating the bare electron mass to an effective mass, and ϵ is the dielectric constant of the semiconductor. In the following (if not explicitly specified otherwise), we will use effective atomic units, defined by $\hbar = e^2/\epsilon = m_e m^* = 1$. In this system of units, the length unit is the Bohr radius a_0 times ϵ/m^* , and the energy has units of Hartrees times m^*/ϵ^2 . As an example, for the GaAs quantum dots, typical values are $\epsilon = 12.4$ and $m^* = 0.067$. The effective Bohr radius a_0^* and effective Hartree H^* are $\simeq 97.93 \text{ \AA}$ and $\simeq 11.86 \text{ meV}$, respectively. In this work, we will consider circular dots only with $N = 2, 6, 12,$ and 20 electrons confined by a parabolic potential $V_{\text{con}}(\mathbf{r}) = m_e m^* \omega^2 r^2/2$. The numbers $N = 2, 6, 12,$ and 20 are so-called magic numbers corresponding to systems with closed harmonic-oscillator shells, and hopefully a single-reference Slater determinant yields a good starting point for our calculations. Although the emphasis here is on closed-shell systems, we show also results for systems with one particle attached to or removed from a closed-shell system for $N = 3, 5, 7, 11,$ and 13 .

The one-body part of our Hamiltonian becomes

$$\hat{H}_0 = \sum_{i=1}^N \left(-\frac{1}{2} \nabla_i^2 + \frac{\omega^2}{2} r_i^2 \right),$$

whereas the interacting part is

$$\hat{V} = \sum_{i<j}^N \frac{1}{|\mathbf{r}_i - \mathbf{r}_j|}.$$

The unperturbed part of the Hamiltonian yields the single-particle energies

$$\epsilon_i = \omega(2n + |m| + 1), \quad (3)$$

where $n = 0, 1, 2, 3, \dots$ and $m = 0, \pm 1, \pm 2, \dots$. The index i runs from $0, 1, 2, \dots$. The shell structure is clearly deduced from this expression. We define R as the shell index. We will denote the shell with the lowest energy as $R = 1$, the shell with the second lowest energy as $R = 2$, and so forth. Hence,

$$R_i \equiv \frac{\epsilon_{i-1}}{\omega} \quad (i = 1, 2, 3, \dots). \quad (4)$$

In the calculations, we limit ourselves to values of $\omega = 0.28$ a.u. (atomic units), $\omega = 0.5$ a.u., and $\omega = 1.0$ a.u. For higher values of the oscillator frequency, the contribution to the energy from the single-particle part dominates over the correlation part. The value $\omega = 1.0$ is an intermediate case, which also allows for comparison with Taut’s exact solution for $N = 2$ (see Ref. 43), while $\omega = 0.5$ and 0.28 represent cases where correlations are stronger, due to the lower average electron density in the dot.

B. Effective interaction

Whenever a single-particle basis is introduced in order to carry out a many-body calculation, it must be truncated. The harmonic-oscillator basis is the *de facto* standard for quantum dots and nuclear structure calculations. In nuclei, the intrinsic Hamiltonian is most easily treated using this basis, and for quantum dots, the confining potential is to a good approximation harmonic.

However, the discrete Hilbert space \mathcal{H} obtained from such a truncation grows exponentially with the number of particles. For example, allowing n single-particle states and N particles,

$$\dim(\mathcal{H}) = \binom{n}{N}.$$

As an example, if we distribute $N = 6$ electrons in the total number of single-particle states defined by 10 major oscillator shells, we have $n = 110$, resulting in $\dim(\mathcal{H}) \approx 2.3 \times 10^{13}$ Slater determinants. This number is already beyond the limit of present full configuration-interaction approaches. In our coupled-cluster calculations, we perform studies up to some 20 major shells. For 20 shells, the total number of single-particle states is $n = 420$, for which $\dim(\mathcal{H}) \approx 1.3 \times 10^{18}$, well beyond reach of standard diagonalization methods in the foreseeable future. For 20 electrons in 20 shells, the number of Slater determinants is much larger, 7.6×10^{33} in total.

But, even if we could run large configuration-interaction calculations, the convergence of the computed energies as a function of the chosen single-particle basis is slow for a harmonic-oscillator basis, mainly due to the fact that this basis does not properly take into account the cusp condition at $|\mathbf{r}_i - \mathbf{r}_j| = 0$ of the Coulomb interaction. In fact, the error ΔE in the energy for a quantum-dot problem, when increasing the dimensionality to one further shell with a harmonic-oscillator (HO) basis, behaves like

$$\Delta E \sim O(R_{\text{HO}}^{-k+\delta-1}). \quad (5)$$

Here, k is the number of times a given wave function Ψ may be differentiated weakly, $\delta \in [0, 1)$ is a constant, and R_{HO} is the last oscillator shell. The derivation of the latter relation is detailed in Ref. 21, together with extensive discussions of the convergence properties of quantum-dot systems. For

the ground state of the two-electron quantum dot, we have precisely $k = 1$, while for higher electron numbers, one observes $k = O(1)$. This kind of estimate tells us that an approximation using only a few HO eigenfunctions necessarily will give an error depending directly on the smoothness k .

Although the coupled-cluster method allows for the inclusion of much larger single-particle spaces, the slow convergence of the energy seen in full configuration-interaction calculations applies to this method as well as it approximates the configuration-interaction solution using the same set of single-particle functions. For an overview of coupled-cluster error analysis, see Refs. 35 and 44.

One way to circumvent the dimensionality problem is to introduce a renormalized Coulomb interaction \hat{V}_{eff} defined for a limited number of low-lying oscillator shells. Such techniques have been widely used in nuclear many-body problems (see, for example, Refs. 15,45 and 46). For quantum dots, this was first applied to a configuration interaction calculation by Navratil *et al.*,⁴⁷ albeit for a different quantum-dot model. But, the potential of this method has not been explored fully, except for recent preliminary studies in Refs. 15,21, and 48, which demonstrate a significant improvement of the eigenvalues. Furthermore, we expect that the potential of this method is of even greater interest when linked up with an efficient many-body method such as the coupled-cluster approach.

The recipe for obtaining such an effective interaction is detailed in several works (see, for example, Refs. 15,46, and 49). Here, we give only a brief overview.

The Hilbert space \mathcal{H} is divided into two parts $P\mathcal{H}$ and $Q\mathcal{H}$, where P and is the orthogonal projector onto the smaller, effective model space, and $Q = 1 - P$. Note here that $P\mathcal{H}$ will be the space in which we do our many-body computations, and \mathcal{H} is, in principle, the *whole untruncated* Hilbert space. The interaction operator \hat{V} is considered a perturbation, and we introduce a convenient complex parameter z and study $\hat{H}(z) = \hat{H}_0 + z\hat{V}$. Setting $z = 1$ recovers the original Hamiltonian.

Consider a similarity transformation of $\hat{H}(z)$ defined by

$$\tilde{H}(z) \equiv e^{-X(z)} \hat{H}(z) e^{X(z)}, \quad (6)$$

where the operator $X(z)$ is such that the property

$$Q\tilde{H}(z)P = 0 \quad (7)$$

holds. Equation (6) must not be confused with equations from coupled-cluster theory. The idea is that $X(z)$ should be determined from perturbation theory, which gives an analytic operator function with $X(0) = 0$.

The most important consequences of these equations are that (i) \tilde{H} have identical eigenvalues with \hat{H} , (ii) that there are $D = \dim(P\mathcal{H})$ eigenvalues, the eigenvectors of which are *entirely in the model space* $P\mathcal{H}$. Thus, the effective Hamiltonian defined by

$$\hat{H}_{\text{eff}}(z) \equiv P\tilde{H}(z)P \quad (8)$$

is a model-space operator with D exact eigenvalues. At $z = 0$, these are the unperturbed eigenvalues, and these are continued analytically as z approaches $z = 1$.

Equations (6) and (7) are not sufficient to determine $X(z)$ uniquely. The order-by-order expansion of $X(z)$ must be supplied with side conditions. One of the most popular

conditions is that $X(z)^\dagger = -X(z)$ such that $\tilde{H}(z)$ is Hermitian, and, additionally, that the effective eigenvectors are *as close as possible to the exact eigenvectors*, i.e., that the quantity Δ defined by

$$\Delta \equiv \sum_{k=1}^D \|\Psi_k - |\Psi_{\text{eff},k}\rangle\|^2 \quad (9)$$

is minimized, where $|\Psi_{\text{eff},k}\rangle$ are the eigenvectors of \hat{H}_{eff} (see Ref. 15). One can obtain a formula for $X(z)$ in this case, namely,

$$X = \text{artanh}(\omega - \omega^\dagger),$$

where $\omega = Q\omega P$ is the operator such that $\exp(\omega)P|\Psi_k\rangle = |\Psi_k\rangle$.

Order-by-order expansion of $\tilde{H}(z)$ reveals that it contains m -body terms for all $m \leq N$, even though \hat{V} only contains two-body interactions. However, the many-body terms can be shown to be of lower order⁴⁹ in z . By truncating $\tilde{H}(z)$ at terms at the two-body level, we obtain the so-called *subcluster approximation* to the effective Hamiltonian. This can be computed by exact diagonalization of the two-body problem, a simple task for the quantum-dot problem.⁵⁰

The one-body part of \tilde{H} is always H_0 , so it is natural to define the effective *interaction* by

$$H_{\text{eff}} = H_0 + V_{\text{eff}}. \quad (10)$$

The reader should, however, keep in mind that the subcluster approximation always produces missing many-body correlations when inserted in a many-body context. The size of this source of error can only be quantified *a posteriori*, either by comparison with experiment and/or exact calculations (see, for example, Ref. 51) for a discussion on missing many-body physics and the nuclear many-body problem.

C. Coupled-cluster method

The single-reference coupled-cluster theory is based on the exponential ansatz for the ground-state wave function of the N -electron system

$$|\Psi_0\rangle = e^T |\Phi_0\rangle,$$

where T is the cluster operator (an N -particle– N -hole excitation operator) and $|\Phi_0\rangle$ is the corresponding reference determinant (defining our chosen closed-shell system or vacuum) obtained by performing some mean-field calculation or by simply filling the N lowest-energy single-electron states in two dimensions.

The operator T is a simple many-body excitation operator, which in all standard coupled-cluster approximations is truncated at a given (usually low) M -particle– M -hole excitation level $M < N$, with N being the number of electrons. If all excitations are included up to the N -particle– N -hole set of Slater determinants, one ends up with solving the full problem. The general form of the truncated cluster operator, defining a standard single-reference coupled-cluster approximation characterized by the chosen excitation level M , is

$$T = T_1 + T_2 + T_3 + \dots + T_M, \quad (11)$$

where

$$T_k = \frac{1}{(k!)^2} \sum_{i_1, \dots, i_k; a_1, \dots, a_k} t_{i_1 \dots i_k}^{a_1 \dots a_k} \hat{a}_{a_1}^\dagger \dots \hat{a}_{a_k}^\dagger \hat{a}_{i_1} \dots \hat{a}_{i_k}.$$

Here and in the following, the indices i, j, k, \dots label occupied single-particle orbitals while a, b, c, \dots label unoccupied orbitals. The unknown amplitudes t_i^a , t_{ij}^{ab} , etc., in the last equation are determined from the solution of the coupled-cluster equations discussed below. For a truncated T operator, we will use the notation $T(M)$, where M refers to highest possible particle-hole excitations.

As an example, we list here the expressions for one-particle–one-hole, two-particle–two-hole, and three-particle–three-hole operators, labeled T_1 , T_2 , and T_3 , respectively,

$$T_1 = \sum_{i < \varepsilon_f} \sum_{a > \varepsilon_f} t_i^a \hat{a}_a^\dagger \hat{a}_i, \quad (12)$$

and

$$T_2 = \frac{1}{4} \sum_{ij < \varepsilon_f} \sum_{ab > \varepsilon_f} t_{ij}^{ab} \hat{a}_a^\dagger \hat{a}_b^\dagger \hat{a}_j \hat{a}_i, \quad (13)$$

and finally

$$T_3 = \frac{1}{36} \sum_{ijk < \varepsilon_f} \sum_{abc > \varepsilon_f} t_{ijk}^{abc} \hat{a}_a^\dagger \hat{a}_b^\dagger \hat{a}_c^\dagger \hat{a}_k \hat{a}_j \hat{a}_i. \quad (14)$$

We will in this paper limit ourselves to a single reference Slater determinant Φ_0 .

The cluster amplitudes $t_{i_1 \dots i_n}^{a_1 \dots a_n}$ are determined by solving a coupled system of nonlinear and energy-independent algebraic equations of the form

$$\langle \Phi_{i_1 \dots i_n}^{a_1 \dots a_n} | \bar{H} | \Phi_0 \rangle = 0, \quad i_1 < \dots < i_n, \quad a_1 < \dots < a_n \quad (15)$$

where $n = 1, \dots, M$. Here,

$$\bar{H} = e^{-T(M)} \hat{H} e^{T(M)} = (\hat{H} e^{T(M)})_C \quad (16)$$

is the similarity-transformed Hamiltonian of the coupled-cluster theory truncated at M -particle– M -hole excitations and the subscript C denotes the connected part of the corresponding operator expression, and $|\Phi_{i_1 \dots i_n}^{a_1 \dots a_n}\rangle \equiv a^{a_1} \dots a^{a_n} a_{i_n} \dots a_{i_1} |\Phi\rangle$ are the n -particle– n -hole or n -tuple excited determinants relative to reference determinant $|\Phi_0\rangle$. The Hamiltonians \bar{H} and \hat{H} are normal ordered.

If we limit ourselves to include only one-particle–one-hole and two-particle–two-hole excitations, what is known as coupled cluster of singles and doubles (CCSD), the method corresponds to $M = 2$, and the cluster operator $T^{(N)}$ is approximated by

$$T(M) = T(2) = T_1 + T_2, \quad (17)$$

given by the operators of Eqs. (12) and (13).

The standard CCSD equations for the singly and doubly excited cluster amplitudes t_a^i and t_{ab}^{ij} , defining T_1 and T_2 , respectively, can be written as

$$\langle \Phi_i^a | \bar{H}(\text{CCSD}) | \Phi_0 \rangle = 0 \quad (18)$$

and

$$\langle \Phi_{ij}^{ab} | \bar{H}(\text{CCSD}) | \Phi \rangle = 0, \quad i < j, \quad a < b \quad (19)$$

where

$$\bar{H}(\text{CCSD}) = \bar{H} = e^{-T(2)} \hat{H} e^{T(2)} = (\hat{H} e^{T(2)})_C \quad (20)$$

is the similarity-transformed Hamiltonian of the CCSD approach and the subscript C stands for connected diagrams only.

The system of coupled-cluster equations is obtained in the following way. We first insert the coupled-cluster wave function $|\Psi_0\rangle$ into the N -body Schrödinger equation

$$\hat{H} |\Psi_0\rangle = \Delta E_0 |\Psi_0\rangle, \quad (21)$$

where

$$\Delta E_0 = E_0 - \langle \Phi_0 | \hat{H} | \Phi_0 \rangle$$

is the corresponding energy relative to the reference energy $\langle \Phi_0 | \hat{H} | \Phi_0 \rangle$, and premultiply both sides on the left by $e^{-T^{(N)}}$ to obtain the connected-cluster form of the Schrödinger equation

$$\bar{H} |\Phi\rangle = \Delta E_0 |\Phi\rangle, \quad (22)$$

where

$$\bar{H} = e^{-T(2)} \hat{H} e^{T(2)} = (H e^{T(2)})_C \quad (23)$$

is the similarity-transformed Hamiltonian.

Next, we project Eq. (22), in which T is replaced by its approximate form $T(M)$ [Eq. (11)] onto the excited determinants $|\Phi_{i_1 \dots i_n}^{a_1 \dots a_n}\rangle$, corresponding to the M -particle– M -hole excitations included in T_M . The excited determinants $|\Phi_{i_1 \dots i_n}^{a_1 \dots a_n}\rangle$ are orthogonal to the reference determinant $|\Phi_0\rangle$, so that we end up with nonlinear and energy-independent algebraic equations of the form of Eq. (15).

Once the system of equations [Eq. (15)] is solved for T_M or $t_{i_1 \dots i_n}^{a_1 \dots a_n}$ [or Eqs. (18) and (19) are solved for T_1 and T_2 or t_a^i and t_{ab}^{ij}], the ground-state coupled-cluster energy is calculated using the equation

$$E_0 = \langle \Phi_0 | \hat{H} | \Phi_0 \rangle + E_0 \Delta = \langle \Phi_0 | \hat{H} | \Phi_0 \rangle + \langle \Phi_0 | \bar{H} | \Phi_0 \rangle. \quad (24)$$

It can easily be shown that if H contains only up to two-body interactions and $2 \leq M \leq N$, we can write

$$E_0 = \langle \Phi_0 | \hat{H} | \Phi_0 \rangle + \langle \Phi_0 | [\hat{H}(T_1 + T_2 + \frac{1}{2}T_1^2)]_C | \Phi_0 \rangle. \quad (25)$$

In other words, we only need T_1 and T_2 clusters to calculate the ground-state energy E_0 of the N -body ($N \geq 2$) system, even if we solve for other cluster components T_n with $n > 2$. As long as the Hamiltonian contains up to two-body interactions, the above energy expression is correct even in the exact case, when the cluster operator T is not truncated (see, for example, Refs. 17, 18, and 30 for proof).

The nonlinear character of the system of coupled-cluster equations of the form of Eq. (15) does not mean that the resulting equations contain very high powers of T_M . For example, if the Hamiltonian \hat{H} does not contain higher-than-pairwise interactions, the CCSD equations for the T_1 and T_2 clusters, or for the amplitudes t_a^i and t_{ab}^{ij} that represent these clusters, become

$$\langle \Phi_i^a | [\hat{H}(1 + T_1 + T_2 + \frac{1}{2}T_1^2 + T_1 T_2 + \frac{1}{6}T_1^3)]_C | \Phi \rangle = 0, \quad (26)$$

$$\langle \Phi_{ij}^{ab} | [\hat{H}(1 + T_1 + T_2 + \frac{1}{2}T_1^2 + T_1T_2 + \frac{1}{6}T_1^3 + \frac{1}{2}T_2^2 + \frac{1}{2}T_1^2T_2 + \frac{1}{24}T_1^4)]_C | \Phi \rangle = 0. \quad (27)$$

The explicitly connected form of the coupled-cluster equations, such as Eqs. (15) or (26) and (27), guarantees that the process of solving these equations leads to connected terms in cluster components of T and connected terms in the energy E_0 , independent of the truncation scheme M used to define T_M . The absence of disconnected terms in T_M and E_0 is essential to obtain the rigorously size-extensive results.^{17,18} It is easy to extend the above equations for the cluster amplitudes to include triples excitations, leading to the so-called CCSDT (Ref. 52) hierarchy of equations. Defining

$$f = \sum_{pq} f_{pq} \{a_p^+ a_q\}$$

with f_{pq} the Fock matrix elements and

$$W = \frac{1}{4} \sum_{pqrs} \langle pq || rs \rangle \{a_p^+ a_q^+ a_r a_s\},$$

where $\langle pq || rs \rangle$ are antisymmetrized two-body matrix elements, the extension to triples gives the following equations for the amplitudes with one-particle–one-hole excitations:

$$\langle \Phi_i^a | [fT_1 + f(T_2 + 1/2T_1^2) + WT_1 + W(T_2 + 1/2T_1^2) + W(T_1T_2 + 1/6T_1^3 + T_3)]_C | \Phi \rangle = 0,$$

and with two-particle–two-hole excitations

$$\langle \Phi_{ij}^{ab} | [fT_1 + f(T_3 + T_2T_1) + W + WT_1 + W(T_2 + 1/2T_1^2) + W(T_1T_2 + 1/6T_1^3 + T_3) + W(T_1T_3 + 1/2T_2^2 + 1/2T_2T_1^2 + 1/24T_1^4)]_C | \Phi \rangle = 0,$$

and, with three-particle–three-hole excitations, we end up with

$$\langle \Phi_{ijk}^{abc} | [fT_3 + f(T_3T_1 + 1/2T_2^2) + WT_2 + W(T_3 + T_1T_2) + W(1/2T_2 + T_3T_1/2T_1^2 + T_1) + W(T_2T_3 + 1/2T_2^2T_1 + 1/2T_3T_1^2 + 1/6T_2T_1^3)]_C | \Phi \rangle = 0.$$

Different approximations to the solution of the triples equations yield different CCSDT approximations. The CCSD method scales (in terms of the most computationally expensive contribution) as $n_o^2 n_u^4$, where n_o represents the number of occupied orbitals and n_u the number of unoccupied single-particle states. The full CCSDT scales as $n_o^3 n_u^5$.

Coupled-cluster theory with inclusion of full triples CCSDT is usually considered to be too computationally expensive in most many-body systems of considerable size. Therefore, triples corrections are usually taken into account perturbatively using the noniterative CCSD(T) approach described in Ref. 53. Recently, a more sophisticated way of including the full triples is known as the Λ -CCSD(T) approach.^{36–39} In the Λ -CCSD(T) approach, the left-eigenvector solution of the CCSD similarity-transformed Hamiltonian is utilized in the calculation of a noniterative triples correction to the coupled-

cluster ground-state energy. The left-eigenvalue problem is given by

$$\langle \Phi_0 | \Lambda \bar{H} = E \langle \Phi_0 | \Lambda, \quad (28)$$

where Λ denotes the de-excitation cluster operator

$$\Lambda = 1 + \Lambda_1 + \Lambda_2, \quad (29)$$

$$\Lambda_1 = \sum_{i,a} \lambda_a^i a_a a_i^\dagger, \quad (30)$$

$$\Lambda_2 = \frac{1}{4} \sum_{i,j,a,b} \lambda_{ab}^{ij} a_b a_a a_i^\dagger a_j^\dagger. \quad (31)$$

The unknowns, λ_a^i and λ_{ab}^{ij} , result from the ground-state solution of the left-eigenvalue problem (28). Using a single-particle basis that diagonalizes the Fock matrix f within the *hole-hole* and *particle-particle* blocks simultaneously, and utilizing the λ_a^i and λ_{ab}^{ij} de-excitation amplitudes together with the cluster amplitudes t_a^i and t_{ij}^{ab} , we get the noniterative Λ -CCSD(T) energy correction to the coupled-cluster correlation energy (see Refs. 36–39 for more details)

$$\Delta E_3 = \frac{1}{(3!)^2} \sum_{ijkabc} \langle \Phi_0 | \Lambda (f_{hp} + W)_N | \Phi_{ijk}^{abc} \rangle \times \frac{1}{\gamma_{ijk}^{abc}} \langle \Phi_{ijk}^{abc} | (W_N T_2)_C | \Phi_0 \rangle. \quad (32)$$

Here, f_{hp} denotes the part of the normal-ordered one-body Hamiltonian that annihilates particles and creates holes, while

$$\gamma_{ijk}^{abc} \equiv f_{ii} + f_{jj} + f_{kk} - f_{aa} - f_{bb} - f_{cc} \quad (33)$$

is expressed in terms of the diagonal matrix elements of the normal-ordered one-body Hamiltonian f . In the case of Hartree-Fock orbitals, the one-body part of the Hamiltonian is diagonal and f_{hp} vanishes. The state $|\Phi_{ijk}^{abc}\rangle$ is a three-particle–three-hole excitation of the reference state. For a further discussion of various approximations to the triples correlations, see, for example, Refs. 17 and 18.

In this paper, we focus on the CCSD, the CCSD(T), and the Λ -CCSD(T) approaches, using either a renormalized or an unrenormalized interaction. In order to avoid an iterative solution of the CCSD(T) and Λ -CCSD(T) equations, we start from a self-consistent Hartree-Fock basis such that the Fock matrix f is diagonal. Using such a basis, the computational cost of the CCSD(T) and Λ -CCSD(T) energy corrections is $n_o^3 n_u^4$ number of cycles, done only once. It is also important to keep in mind, in particular, that when linking our coupled-cluster theory with Monte Carlo approaches, a wave function-based method such as coupled-cluster theory is defined within a specific subset of the full Hilbert space. In our case, the Hilbert space will be defined by all possible many-body wave functions, which can be constructed within a certain number of the lowest-lying single-particle states.

D. Diffusion Monte Carlo

The diffusion Monte Carlo method seeks the solution of the equation

$$\partial_\tau |\Psi(\mathbf{R}, \tau)\rangle = [\hat{H} - E_0] |\Psi(\mathbf{R}, \tau)\rangle, \quad (34)$$

where \mathbf{R} collectively indicates the degrees of freedom of the system (the $3N$ electron coordinates, in this case). By expanding the state $|\Psi(\mathbf{R}, \tau)\rangle$ on the basis of eigenstates $|\phi_n\rangle$ of \hat{H} , a formal solution of Eq. (34) is given by

$$\begin{aligned} |\Psi(\mathbf{R}, \tau)\rangle &= e^{-(\hat{H}-E_0)\tau} |\Psi(\mathbf{R}, 0)\rangle \\ &= \sum_n e^{-(\hat{H}-E_0)\tau} |\phi_n\rangle \langle \phi_n | \Psi(\mathbf{R}, 0)\rangle \\ &= \sum_n e^{-(\hat{E}_n-E_0)\tau} |\phi_n\rangle \langle \phi_n | \Psi(\mathbf{R}, 0)\rangle \end{aligned} \quad (35)$$

from which it is evident that, for $\tau \rightarrow \infty$, the only surviving component is the ground state of \hat{H} . Equation (34) can be numerically solved by expanding the state to be evolved in eigenstates $|\mathbf{R}_i\rangle$ of the position operator (called “walkers”), so that the evolution reads as

$$\sum_i \langle \mathbf{R}_i | \Psi(\mathbf{R}, \tau)\rangle = \sum_i \langle \mathbf{R}_i | e^{-(\hat{H}-E_0)\tau} | \mathbf{R}'_i\rangle \langle \mathbf{R}'_i | \Psi(\mathbf{R}', 0)\rangle. \quad (36)$$

Formally, in terms of the Green’s function solution of Eq. (34), the solution can be written as

$$\Psi(\mathbf{R}, \tau) = \int G(\mathbf{R}', \mathbf{R}, \tau) \Psi(\mathbf{R}', 0) d\mathbf{R}'. \quad (37)$$

The Green’s function $G(\mathbf{R}', \mathbf{R}, \tau) = \langle \mathbf{R} | \exp[-(\hat{H} - E_0)\tau] | \mathbf{R}'\rangle$ is, in general, unknown. However, in the limit $\Delta\tau \rightarrow 0$, it can be written in the following form:

$$G(\mathbf{R}', \mathbf{R}, \tau) \simeq \sqrt{\left(\frac{m_e m^*}{2\pi\hbar^2 \Delta\tau}\right)^d} e^{\frac{(\mathbf{R}-\mathbf{R}')^2}{2\hbar^2/m_e m^* \Delta\tau}} e^{-[V(\mathbf{R})-E_0]\Delta\tau}, \quad (38)$$

that is, as the product of the free-particle Green’s function, having the effect of displacing the d -dimensional walkers, and a factor containing the potential, which is interpreted as a weight for the estimators computed at the walker position, and a probability for the walker itself to generate one or more copies of itself in the next generation. Due to the divergence of the potential at the origin, it is necessary to modify the algorithm, introducing the so-called “importance sampling.” In practice, the sampled distribution is modified by multiplying by an approximate solution of the Schrödinger equation $\Psi_T(\mathbf{R})$, which is usually determined by a variational Monte Carlo calculation

$$\Psi_T(\mathbf{R})\Psi(\mathbf{R}, \tau) = \int G(\mathbf{R}', \mathbf{R}, \tau) \frac{\Psi_T(\mathbf{R})}{\Psi_T(\mathbf{R}')} \Psi_T(\mathbf{R}')\Psi(\mathbf{R}', 0) d\mathbf{R}'. \quad (39)$$

A final important observation is the fact that the procedure described above is well defined only in the case of a totally symmetric ground state. For a many-fermion system, it would be necessary, in principle, to project on an excited state of the Hamiltonian, which leads to a severe instability of the variance on the energy estimation. This problem is usually treated by artificially imposing, as an artificial boundary condition, that the solution vanishes on the nodes of the trial function Ψ_T (fixed-node approximation). Many other technical details enter the real calculation. A thorough description of the diffusion Monte Carlo (DMC) algorithm, as implemented for the calculations of this paper, can be found in Ref. 54.

The fixed-node DMC calculations depend on the quality of the trial wave function $\Psi_T(\mathbf{R})$, which is usually built starting from a parametrized ansatz. The values of the parameters are computed by minimizing the expectation value of the Hamiltonian on $\Psi_T(\mathbf{R})$. The trial wave functions we use have the form¹⁰

$$\Psi(\mathbf{R})_{L,S} = \exp[\phi(\mathbf{R})] \sum_{i=1}^{N_{\text{conf}}} \alpha_i \Xi_i^{L,S}(\mathbf{R}), \quad (40)$$

where the α_i are variational parameters. Because in this paper we are considering only closed-shell dots that have $L = 0$ and $S = 0$, the sum in Eq. (40) reduces to a single term

$$\Xi^{L=0,S=0} = D^\uparrow D^\downarrow, \quad (41)$$

where the D^χ are Slater determinants of spin-up and spin-down electrons, using orbitals from a local density approximation calculation with the same confining potential and the same number of electrons. The function $\exp[\phi]$ in Eq. (40) is a generalized Jastrow factor of the form

$$\begin{aligned} l\phi(\mathbf{R}) &= \sum_{i=1}^N \left[\sum_{k=1}^6 \gamma_k J_0 \left(\frac{k\pi r_i}{R_c} \right) \right] \\ &+ \sum_{i<j}^N \frac{1}{2} \left(\frac{a_{ij} r_{ij}}{1 + b(r_i) r_{ij}} + \frac{a_{ij} r_{ij}}{1 + b(r_j) r_{ij}} \right), \end{aligned} \quad (42)$$

where

$$b(r) = b_0^{ij} + b_1^{ij} \tan^{-1}[(r - R_c)^2/2R_c\Delta]. \quad (43)$$

It explicitly includes one- and two-body correlations and effective many-body correlations via the spacial dependence of $b(r)$. The quantity R_c represents an “effective” radius of the dot, which is optimized in the variational procedure. The b_0 and b_1 parameters depend only on the *relative* spin configuration of the pair ij . The parameters a_{ij} are fixed in order to satisfy the cusp conditions, that is, the condition of finiteness of the local energy $\hat{H}\Psi/\Psi$ for $r_{ij} \rightarrow 0$. For a two-dimensional system, $a_{ij} = 1$ if the electron pair ij has antiparallel spin, and $a_{ij} = 1/3$ otherwise. The dependence of a_{ij} on the relative spin orientation of the electron pair introduces spin contamination into the wave function. However, the magnitude of the spin contamination and its effect on the energy has been shown to be totally negligible in the case of well-optimized atomic wave functions,⁵⁵ and we expect that to be true here as well.

Also, the coefficients γ_k in the one-body term, the coefficients Δ , b_0 , and b_1 in the two-body term, and the coefficients α_i multiplying the configuration state functions are optimized by minimizing the variance of the local energy.⁵⁶

III. RESULTS

We start our discussion with the results for the two-electron system since these can, for certain values of the oscillator frequency, be compared with the exact results of Taut.⁴³ These results are presented in the next section using both a renormalized two-body Coulomb interaction and the bare Coulomb interaction. Thereafter, we present coupled-cluster results with singles and doubles excitations for systems with $N = 6$ and 12 electrons with the bare Coulomb interaction.

The slow convergence as a function of the number of oscillator shells with the bare interaction serves to motivate the introduction of an effective Coulomb interaction. In the main result section, we present CCSD, CCSD(T), and Λ -CCSD(T) results for $N = 6, 12,$ and 20 electrons using an effective two-body Coulomb interaction and compare with diffusion Monte Carlo (DMC) calculations for the same systems.

A. Results for two electrons

In this section, we limit our attention to the two-electron system and compare our DMC results with coupled-cluster calculations with CCSD correlations only. The results presented here serve to demonstrate the reliability of using an effective Coulomb interaction.

The CCSD approach gives the exact eigenvalues for the two-particle system. We have employed a standard harmonic-oscillator basis using the frequencies $\omega = 0.5$ and 1.0 a.u. Our results are listed in Table I. The variable R represents the number of oscillator shells in which the effective interaction case represents the model space for which the effective Coulomb interaction is defined. The calculations labeled CCSD- V represent the results obtained with the unrenormalized or bare Coulomb interaction, while the shorthand CCSD- V_{eff} stands for the results obtained with an effective interaction. Since the latter, irrespective of size of model space (number of lowest-lying oscillator shells in our case) always gives the exact lowest-lying eigenvalues by construction (a similarity transformation preserves always the eigenvalues), these results

TABLE I. Ground-state energies for two electrons in a circular quantum dot within the CCSD approach with (CCSD- V_{eff}) and without (CCSD- V) an effective Coulomb interaction. The diffusion Monte Carlo (DMC) results are also included. For $\omega = 1$, Taut's exact result from Ref. 43 is 3 a.u. All energies are in atomic units. There are no triples corrections for the two-body problem. The variable R represents the number of oscillator shells.

ω	R	CCSD- V	CCSD- V_{eff}	DMC
0.5	2	1.786 914	1.659 772	
	4	1.673 874	1.659 772	
	6	1.667 259	1.659 772	
	8	1.664 808	1.659 772	
	10	1.663 535	1.659 772	
	12	1.662 762	1.659 772	
	14	1.662 244	1.659 772	
	16	1.661 875	1.659 772	
	18	1.661 599	1.659 772	
	20	1.661 378	1.659 772	1.659 75(2)
	1.0	2	3.152 329	3.000 000
4		3.025 232	3.000 000	
6		3.013 627	3.000 000	
8		3.009 237	3.000 000	
10		3.000 895	3.000 000	
12		3.000 654	3.000 000	
14		3.000 505	3.000 000	
16		3.000 406	3.000 000	
18		3.000 335	3.000 000	
20		3.000 282	3.000 000	3.000 00(3)

are unchanged as a function of the number of oscillator shells R . For the two-body problem, coupled-cluster theory at the level of singles and doubles excitations yields the same as exact diagonalization in the same two-particle space. In our case, the number of two-body configurations is given by all allowed configurations that can be constructed by placing two particles in the single-particle orbits defined by the given number of oscillator shells R . For $\omega = 1.0$ a.u., Taut's exact result from Ref. 43 is reproduced. The noninteracting part of the Hamiltonian gives a contribution of 2 a.u. to the ground-state energy, while the two-particle interaction results in 1 a.u.

We notice also that the DMC results agree perfectly (within six leading digits) with our CCSD- V_{eff} calculations. The standard error in the DMC calculations is given in parentheses.

If, on the other hand, we use the bare Coulomb interaction, we see that the convergence of the CCSD- V results as a function of R is much slower and in line with the analysis of Ref. 21 and our discussion in Sec. II B. One needs at least some 16–20 major oscillator shells (between 272 and 420 single-particle states) in order to get a result within three to four leading digits close to the exact answer. The slow convergence of the bare interaction for the two-electron problem may be even more prevalent in a many-body system, in particular, for small values of ω , where correlations are expected to be more important. With more particles, we may expect even worse convergence. In Table II, we present for the case of $\omega = 1.0$ a.u. CCSD results for $N = 6$ and 12 electrons. The bare Coulomb interaction in an oscillator basis is used. The diffusion Monte Carlo results are for $N = 6, 20.1597(2)$ a.u., and for $N = 12, 65.700(1)$ a.u. Using the bare interaction thus results in a slow convergence, as will be demonstrated in the next section. The result of 20.1737 a.u. obtained with an effective Coulomb at the CCSD level for $N = 6$ and $R = 20$ is much closer to the DMC result, as can be seen from Table III. These results serve the aim of motivating the introduction of an effective two-particle interaction. In the next section, we will make further comparisons between our results with and without an effective interaction. In particular,

TABLE II. Ground-state energies for $N = 6$ and 12 electrons in a circular quantum dot within the CCSD approach using the bare Coulomb interaction. All energies are in atomic units. There are no triples corrections. Results are presented for an oscillator frequency $\omega = 1.0$ a.u. The variable R represents the number of oscillator shells. For $N = 12$, the first three shells are filled and there are no results for two shells only.

R	$N = 6$	$N = 12$
2	22.219 813	
3	21.419 889	73.765 549
4	20.421 325	70.297 531
6	20.260 893	66.452 006
8	20.221 750	65.889 324
10	20.216 128	65.887 965
12	20.206 257	65.848 353
14	20.199 986	65.825 018
16	20.195 658	65.809 710
18	20.192 497	65.798 902
20	20.189 900	65.789 460

TABLE III. Ground-state energies for $N = 6$ electrons in a circular quantum dot within various coupled-cluster approximations utilizing an effective Coulomb interaction and the diffusion Monte Carlo (DMC) approach. The coupled-cluster results have been obtained with an effective two-body interaction using a self-consistent Hartree-Fock basis and the CCSD, the CCSD(T), and the Λ -CCSD(T) approaches discussed in the text. E_{HF} is the Hartree-Fock energy, while R stands for the number of major oscillator shells. All energies are in atomic units.

ω	R	E_{HF}	CCSD	CCSD(T)	Λ -CCSD(T)	DMC
0.28	10	7.9504	7.6241	7.6032	7.6064	
	12	7.9632	7.6245	7.6023	7.6057	
	14	7.9720	7.6247	7.6016	7.6052	
	16	7.9785	7.6249	7.6012	7.6048	
	18	7.9834	7.6251	7.6008	7.6046	
	20	7.9872	7.6252	7.6006	7.6044	7.6001(1)
0.5	10	12.1927	11.8057	11.7871	11.7892	
	12	12.2073	11.8055	11.7858	11.7880	
	14	12.2173	11.8055	11.7850	11.7873	
	16	12.2246	11.8055	11.7845	11.7868	
	18	12.2302	11.8055	11.7841	11.7864	
	20	12.2346	11.8055	11.7837	11.7862	11.7888(2)
1.0	10	20.6295	20.1766	20.1623	20.1633	
	12	20.6461	20.1753	20.1602	20.1612	
	14	20.6576	20.1746	20.1589	20.1600	
	16	20.6659	20.1742	20.1580	20.1592	
	18	20.6723	20.1739	20.1574	20.1586	
	20	20.6773	20.1737	20.1570	20.1582	20.1597(2)

we will try to extract convergence criteria for both approaches and link our numerical results with the predictions made by Kvaal in Eq. (5).

B. Results with an effective Coulomb interaction

We present here our final and most optimal results for $N = 6, 12,$ and 20 electrons using the CCSD, the CCSD(T), and the Λ -CCSD(T) approaches. We list the CCSD(T) triples results as well. This method has for a long time been considered as the calculational gold standard in quantum chemistry due to its low computational cost and accuracy. We emphasize, however, that the Λ -CCSD(T) approach is an improvement of the standard CCSD(T) approach, and should therefore be considered as our best and most accurate coupled-cluster calculation in this work. In all calculations, we employ an effective Coulomb interaction and a self-consistent Hartree-Fock basis for different values of the oscillator frequency ω and the model space R . The results are compared with diffusion Monte Carlo calculations.⁵⁷ In addition to the values of $\omega = 1.0$ and 0.5 , which serve more as a reference for earlier calculations, we present results for $\omega = 0.28$ a.u., which corresponds to 3.32 eV, a frequency which should approximate the experimental situation in Ref. 58. The role of correlations is also more important for smaller values of ω , allowing us therefore to test the reliability of our single-reference CCSD and Λ -CCSD(T) calculations. As the system becomes more and more correlated, contributions from clusters beyond the $T(3)$ (beyond three-particle–three-hole correlations) level might become non-negligible. For values of $\omega > 1$, the single-particle part of the Hamiltonian dominates and correlations play a less prominent role.

Our results for $N = 6, 12,$ and 20 electrons are displayed in Tables III, IV, and V, respectively. We present also the

mean-field energies (that is, the Hartree-Fock ground-state energies). These are labeled as E_{HF} in the tables. For all values of ω with $R = 20$ major oscillator shells, our best coupled-cluster results, the Λ -CCSD(T) calculations, are very close to the diffusion Monte Carlo calculations. Even for 10 major shells, the results are close to the DMC calculations, suggesting thereby that the usage of an effective interaction provides a better starting point for many-body calculations. The convergence of the coupled-cluster calculation in terms of the number of major oscillator shells is also better than the results shown in Table II with the bare Coulomb interaction. This discussion will be further elaborated at the end of this section.

In $R = 20$ major shells, the Λ -CCSD(T) results are very close to the DMC results. As an example, consider the $\omega = 1$ results for $N = 6$ in Table III. The CCSD result is 20.1737 a.u., while the Λ -CCSD(T) number is 20.1582 a.u. The corresponding DMC energy is $20.1597(2)$ and very close to our Λ -CCSD(T) result. With $R = 20$ shells, our coupled-cluster calculations are almost converged at the level of the fifth or sixth number after the decimal point. At the end of this section, we discuss the convergence properties of the various coupled-cluster approaches as functions of the number of oscillator shells R .

In Tables III, IV, and V, we see that the CCSD(T) results are in most cases overshooting the diffusion Monte Carlo results. From numerous coupled-cluster studies in quantum chemistry, it has been found that CCSD(T) tends to overestimate the role of triples and thereby often overshoots the exact energy. The Λ -CCSD(T) approach has, on the other hand, been found to give highly accurate correlation energies, and even in some cases performing better than the full CCSDT approach (see Refs. 36–39). This is also consistent with our findings for the CCSD(T) and Λ -CCSD(T) correlation energies in quantum dots.

TABLE IV. Same caption as in Table III except the results are for $N = 12$ electrons.

ω	R	E_{HF}	CCSD	CCSD(T)	Λ -CCSD(T)	DMC
0.28	10	26.3556	25.7069	25.6445	25.6540	
	12	26.3950	25.7066	25.6388	25.6491	
	14	26.4221	25.7074	25.6363	25.6470	
	16	26.4410	25.7081	25.6346	25.6456	
	18	26.4551	25.7085	25.6334	25.6446	
	20	26.4659	25.7089	25.6324	25.6439	25.6356(1)
0.5	10	39.9948	39.2218	39.1659	39.1721	
	12	40.0409	39.2203	39.1599	39.1667	
	14	40.0709	39.2197	39.1565	39.1635	
	16	40.0922	39.2195	39.1543	39.1615	
	18	40.1080	39.2194	39.1527	39.1601	
	20	40.1202	39.2194	39.1516	39.1591	39.159(1)
1.0	10	66.6596	65.7552	65.7118	65.7149	
	12	66.7106	65.7484	65.7017	65.7051	
	14	66.7445	65.7449	65.6961	65.6996	
	16	66.7686	65.7430	65.6926	65.6963	
	18	66.7867	65.7417	65.6903	65.6941	
	20	66.8006	65.7409	65.6886	65.6924	65.700(1)

Let us briefly discuss the error in our coupled-cluster calculations. There are two sources of error, the first coming from the finite size of the single-particle basis, and the other from truncation of the cluster amplitude T at the $T(3)$ excitation level (three-particle–three-hole excitations). We are presently not able to provide a mathematical error estimate on truncations in terms of the number of particle-hole excitation operators in the cluster operator T . However, several studies from quantum chemistry (see Ref. 18 and references therein) and in nuclear physics^{32,34} have shown that the CCSD approach gives about 90% of the correlation energy, while CCSDT gives about 99% of the full correlation energy. Assuming that the DMC results are to be considered as exact results, we

can calculate the percentage of correlation energy our CCSD and Λ -CCSD(T) calculations give for different numbers of electrons N and values ω of the confining harmonic-oscillator potential. In Table VI, we list the amount (in percentage) of correlation energy obtained at the CCSD and Λ -CCSD(T) level; the coupled-cluster calculations were done in a model space of $R = 20$ major oscillator shells.

As we see from Table VI, the CCSD approximation gives 90%, or more, of the full correlation energy, while the Λ -CCSD(T) approximation is at the level of 99%–100% of the full correlation energy for $R = 20$. The CCSD approximation is clearly performing better for larger values ω of the confining potential, but this is expected since the system becomes

TABLE V. Same caption as in Table III except the results are for $N = 20$ electrons.

ω	R	E_{HF}	CCSD	CCSD(T)	Λ -CCSD(T)	DMC
0.28	10	63.2588	62.2851	62.1802	62.1946	
	12	63.2016	62.0772	61.9503	61.9692	
	14	63.2557	62.0634	61.9265	61.9466	
	16	63.3032	62.0646	61.9214	61.9423	
	18	63.3369	62.0656	61.9181	61.9395	
	20	63.3621	62.0664	61.9156	61.9375	61.922(2)
0.5	10	95.2872	94.0870	93.9864	93.9971	
	12	95.3407	93.9963	93.8818	93.8944	
	14	95.4164	93.9921	93.8700	93.8833	
	16	95.4676	93.9904	93.8632	93.8771	
	18	95.5043	93.9895	93.8588	93.8730	
	20	95.5320	93.9891	93.8558	93.8702	93.867(3)
1.0	10	157.4356	156.0128	155.9324	155.9381	
	12	157.5613	155.9868	155.8978	155.9042	
	14	157.6437	155.9740	155.8795	155.8863	
	16	157.7002	155.9669	155.8687	155.8758	
	18	157.7413	155.9627	155.8618	155.8690	
	20	157.7725	155.9601	155.8571	155.8646	155.868(6)

TABLE VI. Percentage of correlation energy at the CCSD level (ΔE_2) and at the Λ -CCSD(T) level (ΔE_3), for different numbers of electrons N and values of the confining harmonic potential ω . All numbers are for $R = 20$.

N	$\omega = 0.28$		$\omega = 0.5$		$\omega = 1.0$	
	ΔE_2	ΔE_3	ΔE_2	ΔE_3	ΔE_2	ΔE_3
6	94%	99%	96%	100%	97%	100%
12	91%	99%	94%	100%	96%	100%
20	90%	99%	93%	100%	95%	100%

less and less correlated for larger values of ω . This shows that our coupled-cluster calculations of circular quantum dots are within or even better than the accuracy seen in different applications in both quantum chemistry and nuclear physics. The fact that the (perturbative inclusions of triples) CCSD(T) and the Λ -CCSD(T) methods work that well even for small values of the oscillator energy, is due to the fact that correlations beyond the Hartree-Fock and CCSD levels are still small, not exceeding 10% of the correlation energy.

As previously discussed, DMC results reported in this paper are still affected by the fixed-node approximation. The extent of the error only depends on the nodal surface of the wave function. Because we use a single product of Slater determinants, given the circular symmetry of the dots considered, the nodes depend only on the set of single-particle functions used. Previous tests performed changing the set of single-particle orbitals show that differences are of the order of one millihartrees or less.¹⁰ The optimization of the Jastrow factor only influences the variance of the energy, which is typically of the order of 0.5% of the total energy. Therefore, for circular quantum dots, we can conclude, assuming that the DMC calculations are as close as possible to the exact energies, that with an effective two-body interaction, a finite basis set of $R = 20$ major oscillator shells, and at most three-particle–three-hole correlations in the cluster amplitude, the remaining many-body effects are almost negligible as we are within 99%–100% of the full correlation energy.

In order to study the role of correlations as a function of the oscillator frequency ω and the number of electrons, we define the relative energy

$$\epsilon = \left| \frac{E_{\text{DMC}} - \langle \hat{H}_0 \rangle}{E_{\text{DMC}}} \right|, \quad (44)$$

where $\langle \hat{H}_0 \rangle$ is the expectation value of the one-body operator, the so-called unperturbed part of the Hamiltonian. For $N = 6$, this corresponds to an expectation value $\langle \hat{H}_0 \rangle = 10\omega$ for the one-body part of the Hamiltonian, while for $N = 12$ and 20, the corresponding numbers are $\langle \hat{H}_0 \rangle = 28\omega$ and $\langle \hat{H}_0 \rangle = 60\omega$, respectively. Assuming that the diffusion Monte Carlo results are as close as possible to the true eigenvalues, the quantity ϵ measures the role of the two-body interaction and correlations caused by this part of the Hamiltonian as functions of ω and N , the number of electrons. The results for ϵ are shown in Fig. 1. Results for $N = 2$ are also included.

We see from this figure that the effect of the two-body interaction becomes increasingly important as we increase the number of particles. Moreover, the interaction is more

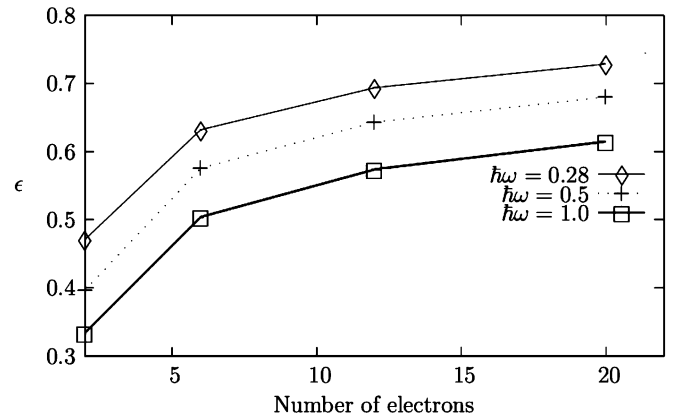


FIG. 1. Relative correlation energy ϵ defined in Eq. (44) for different values of $\hbar\omega$ and number of electrons. The DMC numbers are obtained from Tables I–V using $R = 20$.

important for the smaller values of the oscillator frequency ω . This is expected since the contribution from the one-body operator is reduced due to smaller values of ω . Including more electrons obviously increases the contribution from the two-body interaction. Since our optimal coupled-cluster results are very close to the DMC results, almost identical results are obtained if we replace the DMC results with the Λ -CCSD(T) results.

We can also study the role of correlations beyond the Hartree-Fock energy E_{HF} . In order to do this, we relate the Hartree-Fock energy E_{HF} in Tables III–V to the optimal coupled-cluster calculation, namely, the Λ -CCSD(T) results. The relative difference between these quantities conveys thereby information about correlations beyond the mean-field approximation. This relative measure is defined as

$$\chi = \left| \frac{E_{\Lambda\text{-CCSD(T)}} - E_{\text{HF}}}{E_{\Lambda\text{-CCSD(T)}}} \right|. \quad (45)$$

The results are shown in Fig. 2 for $N = 6, 12,$ and 20. We see from this figure that correlations beyond the Hartree-Fock level are important for few particles and low values of ω . Increasing the number of electrons in the circular dot decreases the role of correlations beyond the mean-field approximation, a feature

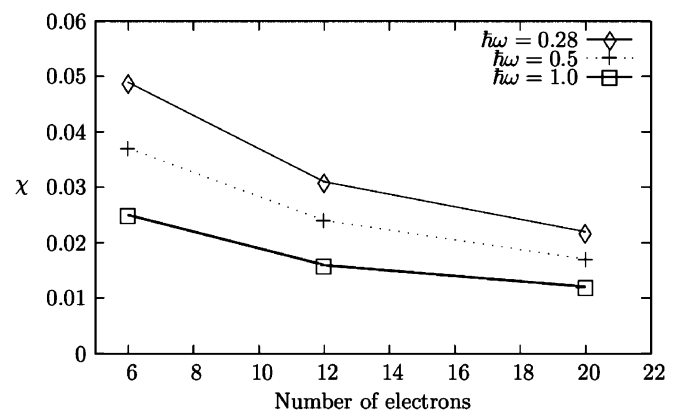


FIG. 2. Relative correlation energy χ defined in Eq. (45) for different values of $\hbar\omega$ and number of electrons. The numbers are obtained from Tables III–V using $R = 20$.

which can be understood from the fact that, for larger systems, multiparticle excitations across the Fermi level decrease in importance. This is due to the fact that the single-particle wave functions for many states around the Fermi level have more than one node, resulting in normally smaller matrix elements. Stated differently, with an increasing number of electrons, the particles close to the Fermi level are more apart from each other, in particular, for those particles that occupy states around and above the Fermi level. The consequence of this is that correlations beyond the Hartree-Fock level decrease in importance when we add more and more particles. This means in turn that, for larger systems, mean-field methods are rather good approximations to systems of many interacting electrons in quantum dots. Similar features are seen in nuclei. For light nuclei, correlations beyond the mean field are very important for ground-state properties, whereas for heavy nuclei such as ^{208}Pb , mean-field approaches provide a very good starting point for studying several observables.

The reader should, however, note that here we have limited our attention to ground-state energies only. Whether our conclusions about the role of correlations pertain to quantities such as, say, spectroscopic factors remains to be studied.

We study now in more detail the convergence properties of our coupled-cluster approaches, in particular, we will relate our Λ -CCSD(T) and CCSD results with the diffusion Monte Carlo results and study the dependence on R . This analysis will be performed with and without an effective Coulomb interaction. The reason for doing this is that we wish to study whether the convergence criterion of Eq. (5), derived for a full configuration-interaction analysis, applies to various coupled-cluster truncations as well. Furthermore, we wish to see whether our calculations with an effective interaction converge faster as a function of R compared to a calculation with the bare interaction.

We compute the following quantities:

$$\log_{10} \epsilon_{\text{CCSD}}(R) = \log_{10} \left| \frac{E_{\text{CCSD}}(R) - E_{\text{DMC}}}{E_{\text{DMC}}} \right| \quad (46)$$

and

$$\log_{10} \epsilon_{\Lambda\text{-CCSD(T)}}(R) = \log_{10} \left| \frac{E_{\Lambda\text{-CCSD(T)}}(R) - E_{\text{DMC}}}{E_{\text{DMC}}} \right|. \quad (47)$$

In Fig. 3, we plot the results for $N = 20$ electrons and $\omega = 0.5$. We have chosen these values since they represent one of the cases where the Λ -CCSD(T) results are always above the DMC results and we have no crossing between these two sets of calculations. The CCSD results, on the other hand, are always, for all cases reported here, above the DMC results. This means that the trend seen in Fig. 3 for the CCSD calculations applies to all cases listed in Tables III–V, while for the Λ -CCSD(T) calculations, these results are similar for all cases except for $N = 6$ and $\omega = 0.5$ and 1.0 ; $N = 12$ and $\omega = 1.0$; and $N = 20$ and $\omega = 1.0$. In these cases, the results at $R = 20$ are slightly below the DMC results. However, the agreement is still excellent. The interesting feature to note in Fig. 3 is that the CCSD results change marginally after $R = 12$ for $N = 20$, and there is essentially very little to gain beyond 20 major shells. With the present accuracy of the DMC results, we can conclude that the CCSD results

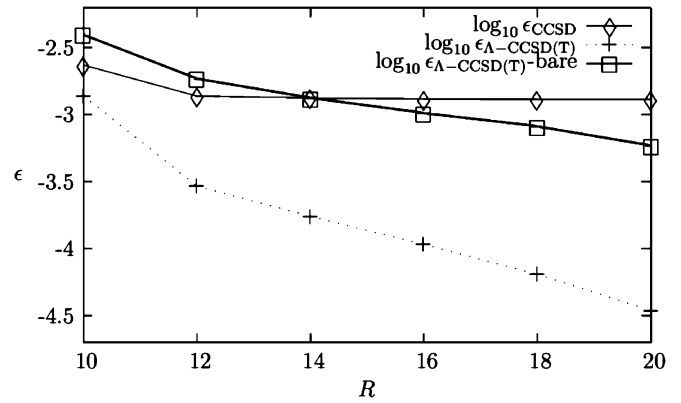


FIG. 3. Relative correlation energy ϵ defined in Eqs. (46) and (47) for different values of R . The values displayed here are for $N = 20$ and $\omega = 0.5$. The numbers are obtained from Table V. We include also the Λ -CCSD(T) results obtained with the bare interaction.

reach, at most, a relative error of approximately 10^{-3} and that it stays almost stable from $R = 12$ shells. The relative error with respect to the Monte Carlo results does not change much. This applies to all CCSD results. This tells us clearly that there are important correlations beyond two-particle–two-hole excitations and that these correlations do not stabilize after some few shells. Furthermore, the slope of the Λ -CCSD(T) calculations is much more interesting and resembles the slope of the configuration interaction analysis of Ref. 21 with an effective interaction. For the ground states of three to five electrons, Kvaal found in Ref. 21 a slope of approximately $\alpha = -4$ to -5 for a parametrization

$$\log_{10} \epsilon \approx c + \alpha \log_{10} R$$

for the ground-state energies of various N -electron quantum dots. The variable c is a constant. Our slopes vary between $\alpha = -4$ and -6 , resulting in a relative error of approximately 10^{-5} at $R = 20$ for the results in Fig. 3. The slope of the Λ -CCSD(T) result is $\alpha = -4.93$. The reader should note that the DMC results can not reach a higher precision. The slope of the CCSD calculation with an effective interaction is $\alpha = -0.67$ after $R = 12$.

In the same figure, we plot also the Λ -CCSD(T) results obtained without an effective Coulomb interaction, that is, with the bare interaction only. These results are labeled as $\log_{10} \epsilon_{\Lambda\text{-CCSD(T)}-\text{bare}}$. A Hartree-Fock basis was used in this case as well in order to obtain converged solutions for the Λ -CCSD(T) equations. We see in this case that the convergence is much slower, resulting in a slope given by $\alpha = -2.58$, a result not far from the analysis of Ref. 21 for the bare interaction. Figure 4 exhibits a similar trend, except that here we present results for $N = 12$ electrons and $\omega = 0.5$. The slope of the Λ -CCSD(T) results is now $\alpha = -6.38$ with an effective interaction and $\alpha = -1.81$ with a bare Coulomb interaction. We notice again that the CCSD results saturate around $R = 12$ major shells. These results are very interesting as they show that the usage of an effective interaction can really speed up the convergence of the energy as a function of the number of shells. Furthermore, these results tell us also that correlations beyond the singles and doubles approach are simply necessary. The convergence behavior of

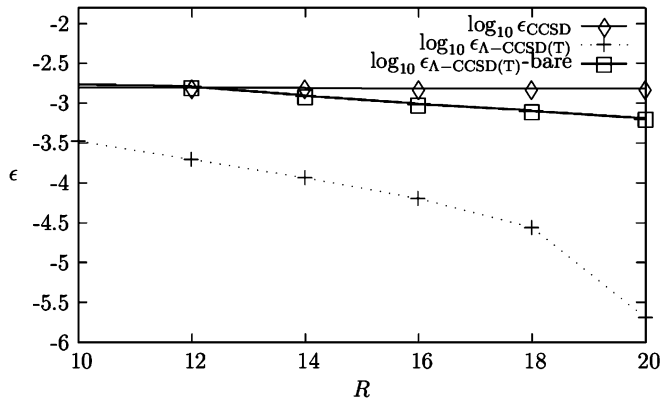


FIG. 4. Relative correlation energy ϵ defined in Eqs. (46) and (47) for different values of R . The values displayed here are for $N = 12$ and $\omega = 0.5$. The numbers are obtained from Table IV. We include also the Λ -CCSD(T) results obtained with the bare interaction.

the Λ -CCSD(T) results resembles, to a large extent, those of a full configuration-interaction approach with and without an effective interaction. Although we can extract similar convergence behaviors as those predicted in Ref. 21 as functions of a truncation in the single-particle basis, the challenge is to provide more rigid mathematical convergence criteria for truncations in the number of particle-hole excitations. Here, we can only justify *a posteriori* that triples corrections are necessary. Work along these lines is in progress.

Using equation-of-motion coupled-cluster method, as discussed in detail in, for example, Refs. 17,18,33, and 34, we can go beyond quantum dots with closed-shell configurations and compute properties such as electrochemical potentials, addition spectra, and excited states. For the sake of completeness, we list in Table VII the electrochemical potentials $\mu(N) = E(N) - E(N - 1)$ for $N = 3, 6, 7, 12,$ and 13 electrons, calculated with the electron attached and ionization potential equation-of-motion coupled-cluster method (CC) and diffusion Monte Carlo (DMC). We have chosen a frequency $\omega = 0.28$, since this frequency is the one that involves the strongest degrees of correlations. It is also the frequency that exhibits the largest deviations between our coupled-cluster results and the diffusion Monte Carlo calculations. We see from Table VII that the agreement between the two different many-body methods is indeed very good, with differences of the order of 0.02 in most cases. The spin assignments for the ground states with both methods are also the same. For $N = 3$, the ground state has orbital momentum projection $M = 1$ and total spin $S = 1/2$; for $N = 5$, the corresponding quantum numbers are $M = 1$ and $S = 1/2$; for $N = 7$, we have $M = 2$ and $S = 1/2$; for $N = 11$, we obtain $M = 0$ and $S = 1/2$; and finally for $N = 13$, we have $M = 3$ and $S = 1/2$. These results demonstrate that the coupled-cluster method can be extended to open-shell systems. With the recent development of two-particle-attached and two-particle-removed coupled-cluster methods (see Ref. 59), we are now in the position where one can also study quantum-dot systems such as $N = 8$ or 18 , or for larger electron systems as well. A more in-depth analysis of our one-particle-attached and one-particle-removed methods will be presented in Ref. 60.

TABLE VII. The electrochemical potentials $\mu(N) = E(N) - E(N - 1)$ for $N = 3, 6, 7, 12,$ and 13 electrons computed with the electron attached and ionization potential equation-of-motion coupled-cluster (CC) method and the diffusion Monte Carlo (DMC) method. A frequency of $\omega = 0.28$ has been used. The absolute value of the energy difference between the two many-body approaches is listed in the final column as $|\Delta E|$. All coupled-cluster results have been obtained for $R = 20$.

	CC	DMC	ΔE
$E(3) - E(2)$	1.2284	1.2123(1)	0.0161(1)
$E(6) - E(5)$	2.0438	2.0663(1)	0.0225(1)
$E(7) - E(6)$	2.4528	2.4341(1)	0.0187(1)
$E(12) - E(11)$	3.5420	3.5618(1)	0.0198(1)
$E(13) - E(12)$	3.8738	3.8582(1)	0.0156(1)

IV. CONCLUSIONS AND PERSPECTIVES

We have shown in this paper that coupled-cluster calculations that employ an effective Coulomb interaction and a self-consistent Hartree-Fock single-particle basis reproduce excellently diffusion Monte Carlo calculations, even for very low oscillator frequencies. This opens up many interesting perspectives, in particular, since our coupled-cluster calculations are rather inexpensive from a high-performance computing standpoint. Properties such as addition spectra and excited states can be extracted using equation-of-motion-based techniques (see, for example, Refs. 17,18,33, and 34). In Refs. 33 and 34, addition spectra of nuclei in the chain of oxygen isotopes have been calculated using the particle-attached or particle-removed equation-of-motion method (Refs. 17 and 18). We have also performed preliminary calculations of addition spectra for quantum dots using the above closed-shell systems for $N = 3, 5, 7, 11,$ and 13 , obtaining a very good agreement with the diffusion Monte Carlo results listed in Refs. 10 and 61. Combining the one-particle-attached and -removed method with our recently developed two-particle-attached and -removed coupled-cluster methods,⁵⁹ we can compute almost all circular quantum dots up $N = 22$ electrons except for dots with $N = 9$ and $N = 15-17$ electrons. These results will be presented elsewhere.⁶⁰

Furthermore, since our codes run in an uncoupled basis, one can also study other trapping potentials than the standard harmonic-oscillator potential. A time-dependent formulation of coupled-cluster theory may even allow for studies of temporal properties of quantum dots such as the effect of a time-dependent perturbation.

For circular dots, we found that with the inclusion of triples correlations, there are, for all systems studied, indications that many-body correlations beyond three-particle-three-hole excitations in the coupled-cluster amplitude T are negligible. We observe also that for systems with more particles, correlations beyond the Hartree-Fock level tend to decrease. Thus, although we are able to extend *ab initio* coupled-cluster calculations of quantum dots to systems up to 50 electrons, a mean-field description will probably convey most of the interesting physics.

With two popular and reliable many-body techniques such as coupled-cluster theory and diffusion Monte Carlo resulting in practically the same energies, one is in the position where one can extract almost exact density functionals for quantum-dot systems. This allows for important comparisons with available density functionals for quantum dots. Finally, we have also noted that triples correlations are necessary in order to obtain correct results. The convergence pattern of our calculations resembles to a large extent those seen in full configuration-interaction calculations.

ACKNOWLEDGMENTS

This work was supported by the Research Council of Norway, by the Office of Nuclear Physics, US Department of Energy (Oak Ridge National Laboratory), and the University of Washington under Contract No. DE-FC02-07ER41457. This research used computational resources of the National Center for Computational Sciences at Oak Ridge National Laboratory, the supercomputing center Titan at the University of Oslo, and the supercomputing center at the University of Trento.

-
- ¹D. Loss and D. P. DiVincenzo, *Phys. Rev. A* **57**, 120 (1998).
²R. Hanson, L. H. Willems van Beveren, I. T. Vink, J. M. Elzerman, W. J. M. Naber, F. H. L. Koppens, L. P. Kouwenhoven, and L. M. K. Vandersypen, *Phys. Rev. Lett.* **94**, 196802 (2005).
³H.-A. Engel, V. N. Golovach, D. Loss, L. M. K. Vandersypen, J. M. Elzerman, R. Hanson, and L. P. Kouwenhoven, *Phys. Rev. Lett.* **93**, 106804 (2004).
⁴C. Fasth, A. Fuhrer, L. Samuelson, V. N. Golovach, and D. Loss, *Phys. Rev. Lett.* **98**, 266801 (2007).
⁵S. Roddaro *et al.*, *Phys. Rev. Lett.* **101**, 18682 (2008).
⁶A. Ambrosetti, J. M. Escartin, E. Lipparini, and F. Pederiva, e-print arXiv:1003.2433.
⁷F. Baruffa, P. Stano, and J. Fabian, *Phys. Rev. Lett.* **104**, 126401 (2010).
⁸A. Harju, *J. Low Temp. Phys.* **140**, 181 (2005).
⁹F. Bolton, *Phys. Rev. B* **54**, 4780 (1996).
¹⁰F. Pederiva, C. J. Umrigar, and E. Lipparini, *Phys. Rev. B* **62**, 8120 (2000).
¹¹L. Colletti, F. Pederiva, and E. Lipparini, *Eur. Phys. J. B* **27**, 385 (2002).
¹²M. Harowitz, D. Shin, and J. Shumway, *J. Low. Temp. Phys.* **140**, 211 (2005).
¹³M. Eto, *Jpn. J. Appl. Phys.* **36**, 3924 (1997).
¹⁴P. A. Maksym and T. Chakraborty, *Phys. Rev. Lett.* **65**, 108 (1990); D. Pfannkuche, V. Gudmundsson, and P. A. Maksym, *Phys. Rev. B* **47**, 2244 (1993); P. Hawrylak and D. Pfannkuche, *Phys. Rev. Lett.* **70**, 485 (1993); J. J. Palacios, L. Martin-Moreno, G. Chiappe, E. Louis, and C. Tejedor, *Phys. Rev. B* **50**, 5760 (1994); T. Ezaki, N. Mori, and C. Hamaguchi, *ibid.* **56**, 6428 (1997).
¹⁵S. Kvaal, *Phys. Rev. C* **78**, 044330 (2008).
¹⁶M. Rontani, C. Cavazzoni, D. Belucci, and G. Goldoni, *J. Chem. Phys.* **124**, 124102 (2006).
¹⁷I. Shavitt and R. J. Bartlett, *Many-Body Methods in Chemistry and Physics* (Cambridge University Press, Cambridge, UK, 2009).
¹⁸R. J. Bartlett and M. Musiał, *Rev. Mod. Phys.* **79**, 291 (2007).
¹⁹T. M. Henderson, K. Runge, and R. J. Bartlett, *Chem. Phys. Lett.* **337**, 138 (2001); *Phys. Rev. B* **67**, 045320 (2003).
²⁰I. Heidari, S. Pal, B. S. Pujari, and D. G. Kanhere, *J. Chem. Phys.* **127**, 114708 (2007).
²¹S. Kvaal, *Phys. Rev. B* **80**, 045321 (2009).
²²A. Kumar, S. E. Laux, and F. Stern, *Phys. Rev. B* **42**, 5166 (1990).
²³M. Fujito, A. Natori, and H. Yasunaga, *Phys. Rev. B* **53**, 9952 (1996).
²⁴H. M. Muller and S. E. Koonin, *Phys. Rev. B* **54**, 14532 (1996).
²⁵C. Yannouleas and U. Landman, *Phys. Rev. Lett.* **82**, 5325 (1999).
²⁶M. Koskinen, M. Manninen, and S. M. Reimann, *Phys. Rev. Lett.* **79**, 1389 (1997).
²⁷K. Hirose and N. S. Wingreen, *Phys. Rev. B* **59**, 4604 (1999).
²⁸P. Gori-Giorgi, M. Seidl, and G. Vignale, *Phys. Rev. Lett.* **103**, 166402 (2009).
²⁹E. Räsänen, S. Pittalis, J. G. Vilhena, and M. A. L. Marques, *Int. J. Quantum Chem.* **110**, 2308 (2010).
³⁰T. U. Helgaker, P. Jørgensen, and J. Olsen, *Molecular Electronic Structure Theory: Energy and Wave Functions* (Wiley, New York, 2000).
³¹G. Hagen, T. Papenbrock, D. J. Dean, and M. Hjorth-Jensen, *Phys. Rev. Lett.* **101**, 092502 (2008).
³²G. Hagen, T. Papenbrock, D. J. Dean, M. Hjorth-Jensen, and B. Velamuri Asokan, *Phys. Rev. C* **80**, 021306 (2009).
³³G. Hagen, T. Papenbrock, and M. Hjorth-Jensen, *Phys. Rev. Lett.* **104**, 182501 (2010).
³⁴G. Hagen, T. Papenbrock, D. J. Dean, and M. Hjorth-Jensen, *Phys. Rev. C* **82**, 034330 (2010).
³⁵R. Schneider, *Numerische Mathematik* **113**, 433 (2009).
³⁶S. A. Kucharski and R. J. Bartlett, *J. Chem. Phys.* **108**, 5243 (1998).
³⁷T. D. Crawford and J. F. Stanton, *Int. J. Quantum Chem.* **70**, 601 (1998).
³⁸A. D. Taube and R. J. Bartlett, *J. Chem. Phys.* **128**, 044110 (2008).
³⁹A. D. Taube and R. J. Bartlett, *J. Chem. Phys.* **128**, 044111 (2008).
⁴⁰P. Navrátil and B. R. Barrett, *Phys. Rev. C* **57**, 562 (1998).
⁴¹P. Navrátil, J. P. Vary, and B. R. Barrett, *Phys. Rev. Lett.* **84**, 5728 (2000).
⁴²R. C. Ashoori, *Nature (London)* **379**, 413 (1996); L. P. Kouwenhoven, T. H. Oosterkamp, M. W. Danoesastro, M. Eto, D. G. Austing, T. Honda, and S. Tarucha, *Science* **278**, 1788 (1997).
⁴³M. Taut, *J. Phys. A: Math. Gen.* **27**, 1045 (1994).
⁴⁴W. Kutzelnigg, *Theor. Chim. Acta* **80**, 349 (1991).
⁴⁵M. Hjorth-Jensen, T. T. S. Kuo, and E. Osnes, *Phys. Rep.* **261**, 125 (1995).
⁴⁶P. Navrátil, S. Quaglioni, I. Stetcu, and B. R. Barrett, *J. Phys. G: Nucl. Part. Phys.* **36**, 08310 (2009).
⁴⁷K. Varga, P. Navrátil, J. Usukura, and Y. Suzuki, *Phys. Rev. B* **63**, 205308 (2001).
⁴⁸S. Kvaal, M. Hjorth-Jensen, and H. M. Nilsen, *Phys. Rev. B* **76**, 085421 (2007).

- ⁴⁹D. J. Klein, *J. Chem. Phys.* **61**, 786 (1974)
- ⁵⁰S. Kvaal, e-print arXiv:0810.2644.
- ⁵¹M. Hjorth-Jensen, D. J. Dean, G. Hagen, and S. Kvaal, *J. Phys. G: Nucl. Part. Phys.* **37**, 064035 (2010).
- ⁵²Y. S. Lee, S. A. Kucharski, and R. J. Bartlett, *J. Chem. Phys.* **81**, 5906 (1984); **82**, 761(E) (1982); J. Noga, R. J. Bartlett, and M. Urban, *Chem. Phys. Lett.* **134**, 126 (1987).
- ⁵³M. J. O. Deegan and P. J. Knowles, *Chem. Phys. Lett.* **227**, 321 (1994).
- ⁵⁴C. J. Umrigar, M. P. Nightingale, and K. J. Runge, *J. Chem. Phys.* **99**, 2865 (1993).
- ⁵⁵C. J. Huang, C. Filippi, and C. J. Umrigar, *J. Chem. Phys.* **108**, 8838 (1998).
- ⁵⁶C. J. Umrigar, K. G. Wilson, and J. W. Wilkins, in *Computer Simulation Studies in Condensed Matter Physics: Recent Developments*, edited by D. P. Landau and H. B. Schüttler (Springer-Verlag, Berlin, 1988); *Phys. Rev. Lett.* **60**, 1719 (1988).
- ⁵⁷Diffusion Monte Carlo calculations for $N = 6$ and 12, with $\omega = 0.28$, have been published in Ref. 10. All the other results have been computed for this paper.
- ⁵⁸S. Tarucha, D. G. Austing, T. Honda, R. J. van der Hage, and L. P. Kouwenhoven, *Phys. Rev. Lett.* **77**, 3613 (1996); *Jpn. J. Appl. Phys.* **36**, 3917 (1997); S. Sasaki, D. G. Austing, and S. Tarucha, *Phys. B (Amsterdam)* **256**, 157 (1998).
- ⁵⁹G. R. Jansen, M. Hjorth-Jensen, G. Hagen, and T. Papenbrock, *Phys. Rev. C* **83**, 054306 (2011).
- ⁶⁰G. Hagen, M. Hjorth-Jensen, S. Kvaal, and F. Pederiva (unpublished).
- ⁶¹A. Ghosal, A. D. Güçlü, C. J. Umrigar, D. Ullmo, and H. U. Baranger, *Phys. Rev. B* **76**, 085341 (2007).